Striatal lateral inhibition regulates action selection in a mouse model of levodopa-induced dyskinesia

Emily L. Twedell[1,2,3,5], Chloe J. Bair-Marshall[2,3,4], Allison E. Girasole[1,2,3,4], Lara K. Scaria[2,3,4], Sadhana Sridhar[2,3,4,5], & Alexandra B. Nelson[1,2,3,4,5]

[1]Neuroscience Graduate Program, UCSF, San Francisco, CA 94158, USA
[2]Kavli Institute for Fundamental Neuroscience, UCSF, San Francisco, CA 94158, USA
[3]Weill Institute for Neurosciences, UCSF, San Francisco, CA 94158, USA
[4]Department of Neurology, UCSF, San Francisco, CA 94158, USA
[5]Aligning Science Across Parkinson's (ASAP) Collaborative Research Network, Chevy Chase, MD 20815, USA
Lead contact
*Correspondence: alexandra.nelson@ucsf.edu

SUMMARY

Striatal medium spiny neurons (MSNs) integrate multiple external inputs to shape motor output. In addition, MSNs form local inhibitory synaptic connections with one another. The function of striatal lateral inhibition is unknown, but one possibility is in selecting an intended action while suppressing alternatives. Action selection is disrupted in several movement disorders, including levodopa-induced dyskinesia (LID), a complication of Parkinson's disease (PD) therapy characterized by involuntary movements. Here, we identify chronic changes in the strength of striatal lateral inhibitory synapses in a mouse model of PD/LID. These synapses are also modulated by acute dopamine signaling. Chemogenetic suppression of lateral inhibition originating from dopamine D2 receptor-expressing MSNs lowers the threshold to develop involuntary movements *in vivo*, supporting a role in motor control. By examining the role of lateral inhibition in basal ganglia function and dysfunction, we expand the framework surrounding the role of striatal microcircuitry in action selection.

INTRODUCTION

Motor control and action selection are coordinated via basal ganglia circuitry. As the input nucleus of the basal ganglia, the striatum integrates excitatory input from the cortex and neuromodulatory input from midbrain dopamine neurons. The striatum consists primarily of GABAergic projection neurons, also known as medium spiny neurons (MSNs).[1,2] MSNs can be divided into two subpopulations: dopamine D1 receptor-expressing (D1-MSN) and D2 receptor-expressing (D2-MSN) neurons. D1- and D2-MSNs are coactivated during movement initiation,[3,4,5,6] but some studies have identified distinct functions in action selection and motor learning.[4,5,7,8,9] One parsimonious model is that ensembles of D1-MSNs facilitate a desired behavior while related ensembles of D2-MSNs suppress competing behaviors.[10,11]

One way to investigate the mechanisms of action selection is to study the circumstances in which it fails. Impaired action selection is a key feature of many movement disorders. One example is levodopa-induced dyskinesia (LID), a complication of Parkinson's disease (PD) in which treatment with the dopamine precursor levodopa results in abnormal, involuntary movements. Prior studies suggest aberrant coordination of D1- and D2-MSN activity in PD/LID, including abnormally high activity in D1-MSNs, larger movement-related D1-MSN ensembles, and suppressed D2-MSN activity with levodopa treatment.[12,5,13]

How are active ensembles of D1-MSNs and D2-MSNs shaped at the synaptic level? Within the striatum, MSNs receive several inhibitory inputs, including from local GABAergic interneurons, and from other MSNs.[14,15,1,16,17] The potential impact of MSN-MSN lateral inhibition has been questioned due to low connection rates and small unitary inhibitory currents.[18] However, since MSNs represent 95% of all striatal neurons, these connections may collectively have a significant impact on circuit function. Despite the anatomical identification of these "lateral" (MSN-MSN) synapses decades ago, their function *in vivo* remains unknown. In sensory systems, lateral inhibition plays a role in improving sensory perception by shaping the pattern of neural activity evoked by sensory stimuli.[19,20,21,22,23,24,25,26] Here, we propose a parallel role in the motor system: striatal lateral inhibition may help coordinate D1- and D2-MSN activity to select an intended behavior while simultaneously suppressing alternatives.[11]

To understand how striatal lateral inhibition shapes action selection, we used *ex vivo* electrophysiology and chemogenetics in a mouse model of PD/LID. We found remodeling of D2- and D1-MSN lateral connections onto D1-MSNs in the mouse model of PD/LID. Chemogenetic inhibition of D2-mediated striatal lateral inhibition lowered the threshold for dyskinesia. Together, these findings provide mechanistic insight into the role of MSN-MSN striatal lateral inhibition in shaping action selection in health and disease.

RESULTS

Striatal lateral connections between MSNs are asymmetric

To study MSN-MSN inhibitory synaptic connections, we employed an optogenetic strategy.[27] We injected a Cre-dependent channelrhodopsin into the dorsolateral striatum (DLS) of A2a-Cre;Drd1-tdTomato or Drd1-Cre;Drd1-tdTomato mice (Figure 1A). In D1-Cre mice, D1-MSN to D1-MSN (D1-D1) and D1-MSN to D2-MSN (D1-D2) connections can be assayed, while in A2a-Cre mice, D2-MSN to D1-MSN (D2-D1) and D2-MSN to D2-MSN (D2-D2) connections can be assayed. We prepared acute brain slices containing

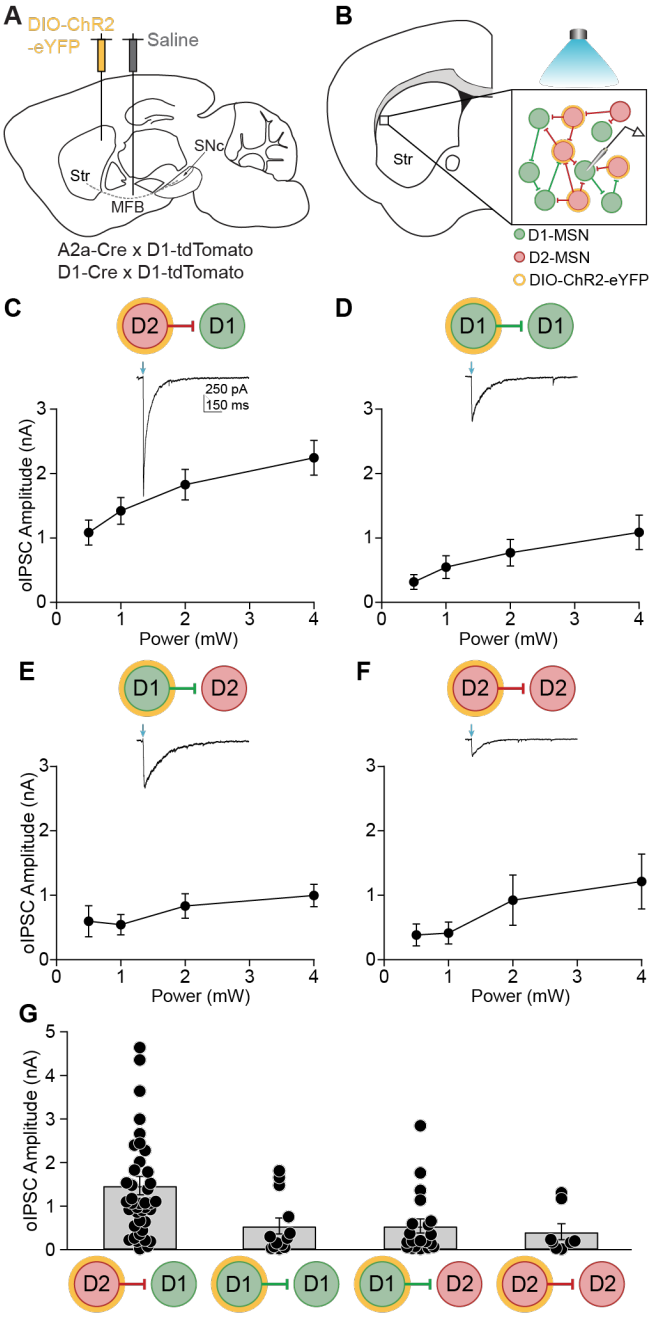

Figure 1. Striatal MSN-MSN synaptic connectivity is asymmetric.
(A) Sagittal schematic showing DIO-ChR2-eYFP injection into the dorsolateral striatum (DLS) and saline injection into the medial forebrain bundle (MFB). **(B)** Coronal schematic depicting an *ex vivo* slice containing the DLS. *Inset*: In this example depicting an A2a-Cre; D1-tdTomato mouse, a whole-cell recording of a medium spiny neuron (D1-MSN, green) is made. Synaptic currents were optically evoked from local D2-MSN (red) collaterals expressing ChR2 (yellow). **(C)** – **(F)** Average oIPSC amplitude evoked by 0.5, 1, 2, and 4 mW light pulses. *Insets*: Representative oIPSCs recorded from MSNs during optical activation of local collaterals. (C) D2-D1 (N = 10, n = 38). (D) D1-D1 (N = 4, n = 14). (E) D1-D2 (N = 8, n = 19). (F) D2-D2 (N = 5, n = 9). **(G)** Average oIPSC amplitude in response to 1 mW optical stimulation for all MSN-MSN connection types. D2-D1: N = 12, n = 41; D1-D1: N = 4, n = 13; D1-D2: N = 9, n = 20; D2-D2: N = 5, n = 8. KW: p = 0.0003. Each dot represents data from one neuron. N = animals; n = cells. Data shown as mean ± SEM.

the striatum and performed whole-cell voltage-clamp recordings of D1-MSNs (tdTomato-positive) or D2-MSNs (tdTomato-negative) in the DLS (Figure 1B). Optical stimulation evoked inhibitory postsynaptic currents (oIPSCs), which represent the sum of local lateral inhibitory inputs onto the post-synaptic neuron (Figure 1C, inset). These oIPSCs were $GABA_A$-dependent, as they were blocked by picrotoxin (S1A-B). oIPSCs were evoked at several light powers and compared across the four MSN-MSN connection types (Figure 1C-F). A prior study of paired recordings found that MSN-MSN connections were asymmetric; those arising from D2 neurons had higher connection strengths.[18] Consistent with these findings, we found that D2-D1 oIPSCs had the highest amplitudes (Figure 1G). There were no significant differences in oIPSC amplitude across the other MSN-MSN connection types. These experiments indicate that the optical approach can recapitulate the asymmetry in MSN-MSN synaptic connectivity, with D2-D1 lateral inhibition being the strongest.

D2-D1 striatal lateral connections are remodeled in parkinsonian animals and parkinsonian animals chronically treated with levodopa

Loss of dopamine in the parkinsonian state and treatment with chronic levodopa trigger significant changes in basal ganglia activity.[28] These alterations in activity are thought to drive homeostatic changes in excitability and synaptic connectivity.[29,30,31,32,33] We

hypothesized that this homeostatic regulation may also take place within the striatal lateral inhibitory network.

To understand how lateral inhibition may contribute to impaired action selection, we tested MSN-MSN connectivity in a mouse model of Parkinson's disease (PD) and levodopa-induced dyskinesia (LID). Both conditions are characterized by abnormal action selection: in PD there is suppression of intended motor programs, resulting in bradykinesia; in LID there is a failure to suppress alternative motor programs, resulting in involuntary movements. To model these disorders, we used the 6-OHDA mouse model of PD. The neurotoxin 6-OHDA was injected unilaterally in the medial forebrain bundle (Figure 2A), resulting in severe dopamine depletion (Figure 2B). Control animals were injected intracranially with saline. Animals recovered for several weeks, after which they were randomized to daily intraperitoneal (IP) injections of levodopa or saline (Figure 2C). 6-OHDA treated animals (Park and LD OFF) exhibited a reduction in movement velocity and an ipsilesional rotational bias (Figure 2D; S2). Parkinsonian animals injected with levodopa (5 mg/kg; LD ON) showed increased movement velocity, contralateral rotation bias, and dyskinesia (Figure 2D-E; S2). In response to each levodopa injection, animals developed abnormal

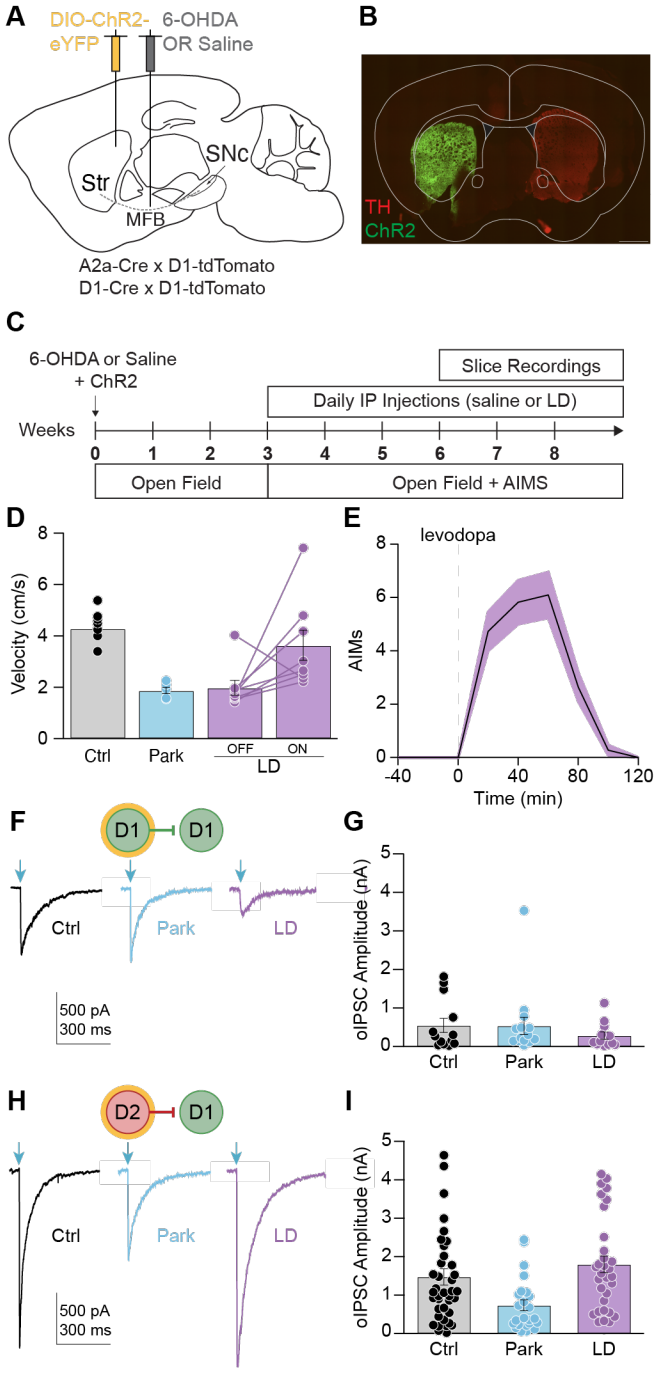

Figure 2. ***Dopamine depletion and chronic levodopa treatment remodel D2-D1 striatal lateral connections.*** **(A)** Sagittal schematic showing DIO-ChR2-eYFP injection into the dorsolateral striatum (DLS) and 6-OHDA or saline injection into the medial forebrain bundle (MFB). **(B)** Representative coronal section of the DLS showing DIO-ChR2-eYFP expression and loss of TH immunoreactivity in the ipsilesional hemisphere of a 6-OHDA-treated mouse. Scale bar is 1 mm. **(C)** Experimental timeline. **(D)** Average velocity in the open field. Ctrl: N = 9; Park: N = 5; LD: N = 8. **(E)** Average abnormal involuntary movement score (AIMs) in response to IP injection of 5 mg/kg levodopa. LD: N = 11. **(F)** Representative D1-D1 oIPSCs recorded from animals in Ctrl (*left*), Park (*middle*), and LD (*right*) groups. **(G)** Average D1-D1 oIPSC amplitude in response to 1 mW optical stimulation for Ctrl (N = 4, n = 13), Park (N = 6, n = 15), and LD (N = 7, n = 12) groups. KW: p = 0.5071. **(H)** Representative D2-D1 oIPSC recorded from animals in Ctrl (*left*), Park (*middle*), and LD (*right*) groups. **(I)** Average D2-D1 oIPSC amplitude in response to 1 mW optical stimulation for Ctrl (N = 12, n = 41), Park (N = 6, n = 24), and LD (N = 8, n = 32) groups. KW: p = 0.0006. Each overlaid dot represents one cell (G, I). N = animals; n = cells. Data shown as mean ± SEM.

involuntary movements (AIMs) which lasted 60-100 minutes, after which animals resumed baseline movement (Figure 2E). These manipulations yielded 3 key experimental groups for subsequent slice electrophysiology (MFB injection/Daily IP injection): Control (saline/saline), Park (6OHDA/saline) and LD (6OHDA/LD).

In the striatum, dopamine depletion leads to decreased D1-MSN activity.[12,5] We hypothesized that this hypoactivity may lead to homeostatic downregulation of inhibitory connections onto D1-MSNs. Indeed, a study of paired recordings found D2-D1 and D1-D1 inhibitory responses to be markedly reduced in parkinsonian animals.[18] To determine whether these connections are also weakened using the optical approach, we compared lateral inhibition in brain slices made from healthy and parkinsonian animals. We did not detect a significant decrease in D1-D1 synaptic strength in the Park condition (Figures 2F-G). Consistent with our hypothesis, oIPSC amplitudes were reduced for D2-D1 connections in Park animals relative to Ctrl (Figures 2H-I).

In mouse models of PD, the activity of D2-MSNs is marginally, if at all, increased.[12,5] Thus, homeostatic changes in lateral inhibition on to D2-MSNs may not be recruited. Due to low connection rates in healthy animals, Taverna et al. were unable to assess D1-D2 connections in the parkinsonian state.[18] Here, we measured D1-D2 connectivity using the optical approach, finding no significant difference across groups (Figure S3A-B).

Less is known about homeostatic changes to synaptic strength in parkinsonian animals chronically treated with levodopa. D1-MSNs are hyperactive in rodent and non-human primate models of LID.[12,5,34,13,35,36] We hypothesized that chronic treatment with levodopa may result in increased D2-D1 lateral inhibition to counteract excessive D1-MSN activity. To determine whether lateral inhibition onto D1-MSNs is altered by dopamine depletion and chronic levodopa treatment, we again used the optical approach. Brain slices were made 24h after the last IP treatment. As predicted, D2-D1 oIPSC amplitudes were restored to control levels in LD animals (Figures 2H-I). We did not detect a change in D1-D1 or D1-D2 synaptic strength in the LD condition (Figures 2F-G, Figure S3A-B). These experiments indicate that lateral inhibition onto D1-MSNs is reduced by dopamine depletion, and that chronic levodopa treatment restores D2-D1 connections.

D2-D1 synaptic responses are inhibited by acute dopamine signaling

Chronic changes in neural activity resulting from dopamine depletion and replacement may drive homeostatic changes in synaptic connectivity. However, these changes may be maladaptive, creating vulnerability to acute changes in striatal dopamine. The previous experiments captured chronic changes in lateral inhibition, but do not recapitulate the acute effects of dopamine signaling. In LID, dyskinesia typically occurs at “peak-dose”, when brain levels of dopamine are elevated; as levodopa wears off, dyskinesia also resolves (Fig 2E).[37] Prior work indicates that dopamine acutely inhibits the amplitude of lateral inhibitory responses in *ex vivo* slices.[38,39,18,27] These observations led to the hypothesis that acute levodopa treatment would lead to a reduction in the amplitude of D2-D1 synaptic responses.

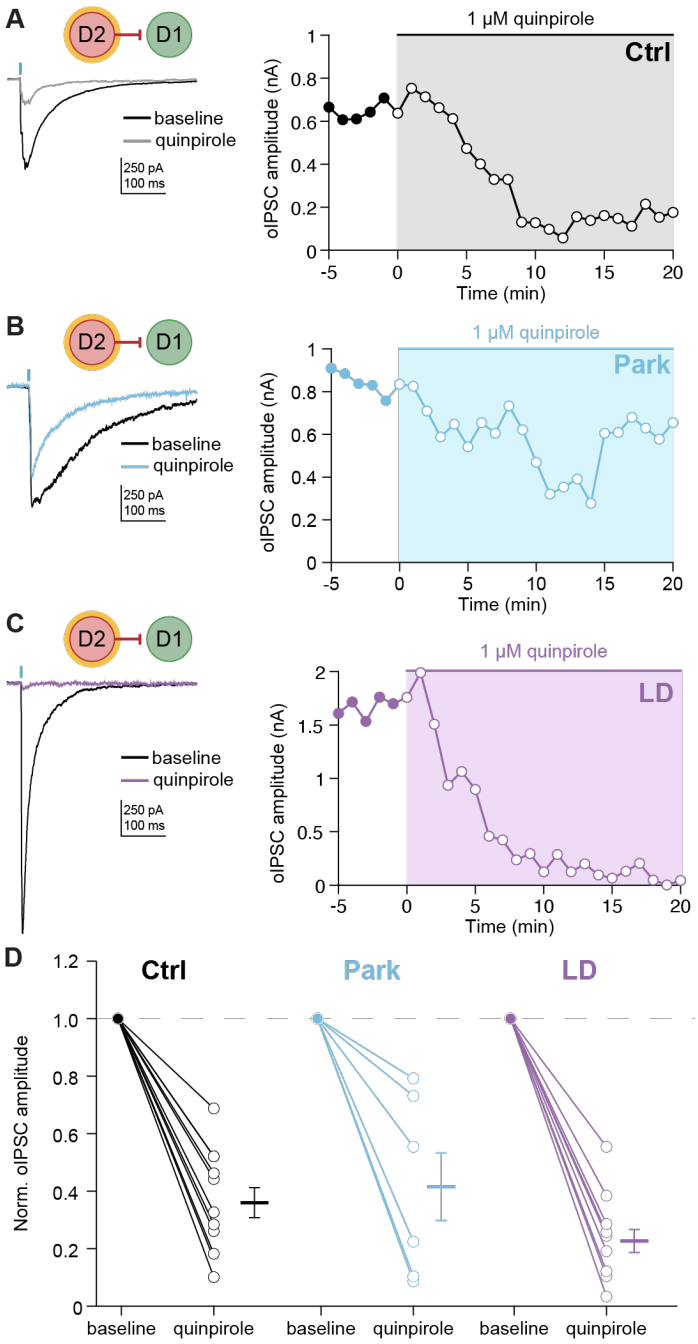

Figure 3. ***Dopamine signaling acutely inhibits D2-D1 synaptic responses.***
(A) - (C) (*Left*) Representative D2-D1 oIPSCs in Ctrl (A), Park (B), and LD (C) groups, before and after application of quinpirole (1 μM). (*Right*) Time course of the effect of quinpirole on D2-D1 oIPSC amplitudes. **(D)** Summary of D2-D1 oIPSC amplitudes before and after quinpirole application in Ctrl (N = 6, n = 11, p = 0.001), Park (N = 4, n = 7, p = 0.0156), and LD (N = 3, n = 9, p = 0.0039) groups. KW: p = 0.2055. N = animals; n = cells. Data shown as mean ± SEM.

To test the effect of acute dopamine signaling on striatal lateral inhibition, we bath-applied the D_2-agonist quinpirole while recording D2-D1 oIPSCs. We found that oIPSCs were acutely reduced by the agonist across all conditions (Figure 3A-D). Taken together, these experiments demonstrate that in parkinsonian/levodopa-treated (LD) animals, acute dopamine signaling inhibits D2-D1 synaptic responses, which may in turn contribute to disinhibition of D1-MSNs *in vivo*.

Chemogenetic inhibition of D2-MSN-mediated striatal lateral inhibition lowers the threshold for levodopa-induced dyskinesia

While these results show alterations in striatal lateral inhibition in *ex vivo* brain slices, we next aimed to test how lateral inhibition contributes to motor output *in vivo*. More specifically, we hypothesized that the largest source of lateral inhibition, D2-D1 connections, facilitate normal action selection by inhibiting competing motor programs. Conversely, we hypothesized that a reduction in D2-D1 synaptic strength might lower the threshold for involuntary movements, as in LID. To date, it has been difficult to differentiate the effect of D2-MSNs on their intrastriatal (e.g., D1-MSNs) and extrastriatal (e.g., globus pallidus pars externa, GPe) targets, making it challenging to isolate the contribution of striatal lateral inhibition to motor output. To address this challenge, we employed a chemogenetic strategy. The inhibitory DREADD hM4D(G_i) can work in two ways: (1) by pre-synaptic inhibition of release and, (2) by reducing excitability via G-

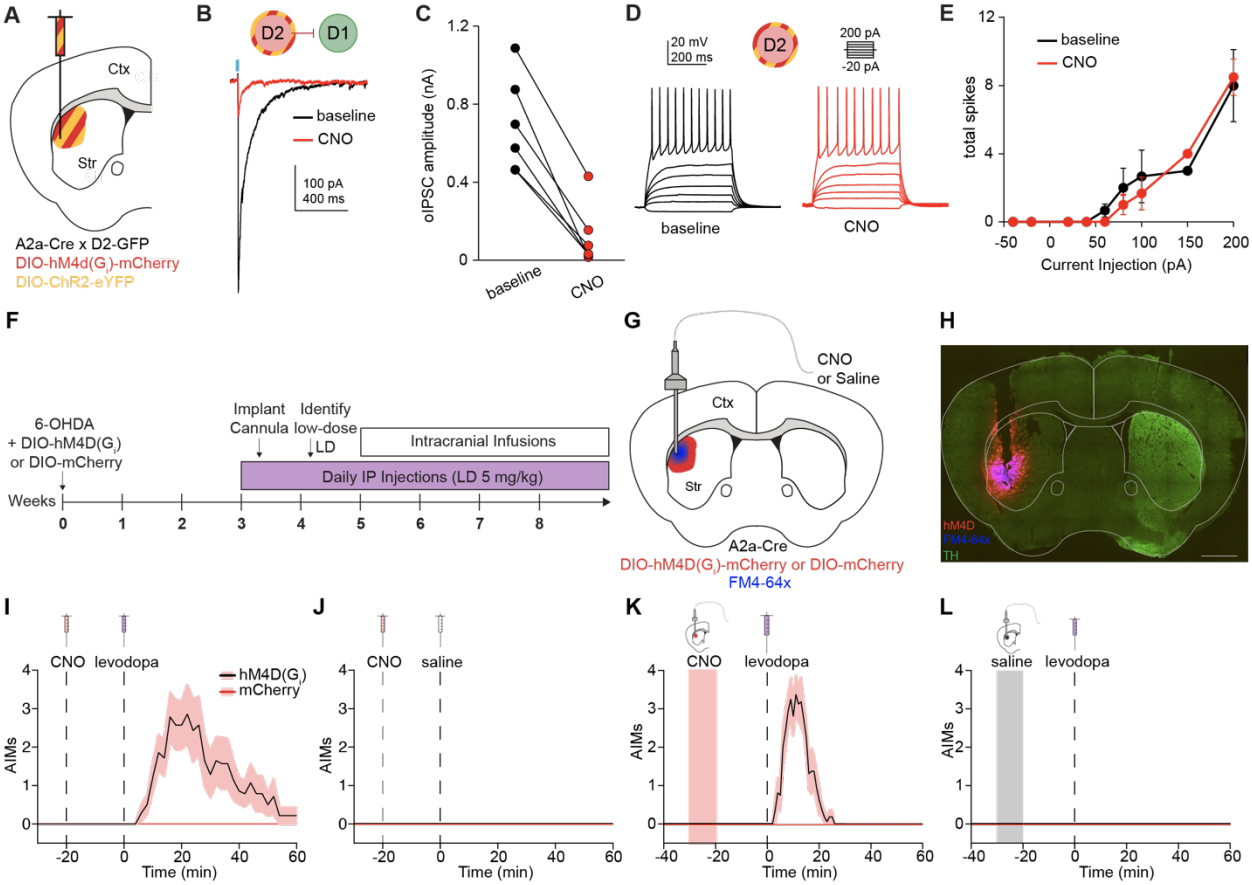

Figure 4. Chemogenetic inhibition of striatal lateral connections originating from D2-MSNs lowers the threshold for levodopa-induced dyskinesia.
(A) Coronal schematic depicting co-injection of DIO-hM4D(G_i)-mCherry and DIO-ChR2-eYFP in the DLS of an A2a-Cre x D2-GFP mouse. **(B)** Representative example of D2-D1 oIPSC before and after application of CNO. **(C)** Summary of changes in D2-D1 oIPSC amplitude with CNO application. N = 2, n = 6. p = 0.0312. **(D)** Example firing rate of a D2-MSN in response to 500 ms steps of current injection before and after CNO application. **(E)** Summary current/firing (I/F) curves of D2-MSNs before and after CNO application. N = 2, n = 3. **(F)** Experimental timeline. **(G)** Coronal schematic showing DIO-hM4D(G_i)-mCherry or DIO-mCherry injection into the dorsolateral striatum (DLS) with local cannula infusion of clozapine-N-oxide (CNO) or saline. FM4-64 dye infused prior to sacrifice. **(H)** Coronal section showing loss of TH immunoreactivity in the ipsilesional hemisphere, expression of DIO-hM4D(G_i)-mCherry, and infusion radius (FM4-64x). Scale bar is 1 mm. **(I)** Average dyskinesia as measured by the Abnormal Involuntary Movement (AIM) score following IP injection of CNO and IP injection of a low dose of levodopa in animals expressing DIO-hM4D(G_i)-mCherry or DIO-mCherry. 2-Way RM ANOVA: p = 0.0059. **(J)** No dyskinesia was observed following IP injection of CNO and IP injection of levodopa. **(K)** Average AIMs following local striatal infusion of CNO and IP injection of a low-dose of levodopa in animals expressing DIO-hM4D(G_i)-mCherry or DIO-mCherry. 2-Way RM ANOVA: $p < 0.0001$. **(L)** No dyskinesia was observed following local striatal infusion of saline and IP injection of a low-dose of levodopa hM4D(G_i): N = 14, mCherry: N = 12. N = animals. Data shown as mean ± SEM.

protein-coupled inwardly rectifying potassium channels (GIRKs).[40,41,42] MSNs, however, do not express GIRKs,[43,44] and thus local striatal activation of hM4D(G_i) would be predicted to reduce local synaptic release (lateral inhibition) without changing the excitability/firing rate of the MSNs. Indeed, we validated this approach using slice electrophysiology, finding that while CNO markedly reduced the amplitude of D2-D1 oIPSCs (Fig 4A-C), it did not change the excitability of D2-MSNs (Fig. 4D-E). Using this approach *in vivo*, we hoped to isolate the role of striatal lateral inhibition in mediating LID.

Implementing this strategy, unilateral 6-OHDA-treated A2a-Cre mice were injected with either a Cre-dependent inhibitory DREADD (DIO-hM4D(G_i)-mCherry) or an inert fluorophore control (DIO-mCherry) into the ipsilateral DLS (Figure 4F). After a period of

recovery, animals began daily levodopa treatments. Later, an infusion cannula was implanted into the DLS to allow for local striatal delivery of the ligand CNO (or saline). At the end of all experiments, a lipophilic dye (FM4-64X) was infused just prior to sacrifice and used to confirm patency of the cannula in postmortem tissue (Figure 4G-H).

To assess the role of D2-mediated lateral inhibition in LID, we first sought to identify a low dose of levodopa (0.75-2 mg/kg) that increased movement (alleviated bradykinesia), but did not evoke dyskinesia. We anticipated we would be able to detect changes in the threshold for dyskinesia at this dose. Prior work suggests that chemogenetic stimulation of D2-MSNs abolishes the therapeutic response to levodopa in parkinsonian mice.[45] To investigate how chemogenetic inhibition of D2-MSNs impacts dyskinesia expression, we delivered an IP injection of CNO followed by an IP injection of low-dose levodopa or saline. As predicted, a reduction of D2-MSN-mediated inhibition with CNO evoked dyskinesia (Figure 4I), while CNO paired with saline did not (Figure 4J).

While systemic administration of CNO in hM4D(G_i)-expressing A2a-Cre animals provides further evidence for the role of D2-MSNs in shaping LID, this manipulation does not isolate the contribution of striatal lateral connections, as hM4D(G_i)-positive terminals are present in both the striatum and the GPe. To determine if suppression of just the D2-MSN-mediated lateral inhibition lowers the threshold for LID, we infused CNO in the DLS, followed by an IP injection of a low-dose of levodopa. Under these conditions, hM4D(G_i)-expressing mice became dyskinetic, while mCherry controls did not (Figure 4K). We performed several additional control experiments: animals expressing hM4D(G_i) or mCherry did not develop abnormal involuntary movements to any other treatment pairing (striatal infusion/IP injection): saline/levodopa (Figure 4L), CNO/saline (Figure S4A), or saline/saline (Figure S4B). These *in vivo* experiments suggest that loss of D2-MSN-mediated lateral inhibition, combined with acute dopamine signaling, can contribute to LID.

DISCUSSION

Despite a long-standing appreciation of striatal MSN-MSN connections from an anatomical perspective, the functional relevance of these connections remains unknown. Here, we used *ex vivo* and *in vivo* techniques to shed light on the role of these connections in both health and disease. Our overarching hypothesis was that these connections help define functional striatal ensembles of MSNs that are activated in conjunction with a specific action. Disruption of these connections might contribute to involuntary movements.

In *ex vivo* brain slices, paired recordings across MSN-MSN subtypes provides critical information about the rate of connectivity and the strength of unitary connections.[18,46] However, this approach is low throughput: depending on the connection type, up to 94% of MSN-MSN pairs lack a 1:1 connection.[18] To overcome this obstacle, we employed an optogenetic approach[27] that allowed us to more comprehensively assess all MSN-MSN connection types. Using this technique, we reproduced the finding from paired recordings that MSN-MSN connections are asymmetric, with D2- to D1-MSN connections being the

strongest overall. A limitation of the optical approach is that it yields a single number (compound inhibitory postsynaptic response amplitude), which likely reflects both the size of unitary responses and connection probability. Despite this limitation, our findings suggest the optical approach is an effective and efficient method for measuring the overall strength of MSN-MSN lateral inhibition.

We next sought to examine how MSN-MSN lateral inhibition is changed across disease states. A previous study using paired recordings found decreased strength of lateral inhibition onto D1-MSNs in the parkinsonian state, with no detectable D1-D1 connections.[18] Consistent with these findings, we observed a decrease in the strength of D2-D1 oIPSC amplitudes. Importantly, the optical approach allowed us to record functional D1-D1 oIPSCs from parkinsonian animals. This finding suggests that although there is a marked reduction in the D1-D1 rate of connectivity, a modest network of D1-D1 connections remains in the parkinsonian state.

High striatal firing rates have been observed in LID across several animal models.[12,5,34,35,36] Further, movement-associated D1-MSN ensembles are larger in parkinsonian animals acutely treated with levodopa.[13] However, we do not understand the microcircuit mechanisms which may lead to the recruitment of large and hyperactive movement-related ensembles in LID. The present study tested the hypothesis that homeostatic changes in MSN-MSN connectivity might create vulnerability to acute dopamine signaling, leading to LID. Consistent with this prediction, we observed a restoration in D2-D1 inhibition. This rebound likely represents a homeostatic response to dopamine replacement therapy, as has been seen in the intrinsic properties of MSNs in the same mouse model.[29]

LID only occurs when levodopa is administered; our initial slice experiments did not capture this acute period of elevated dopamine signaling. To mimic elevated dopamine signaling in *ex vivo* slices, we bath applied the D2R-agonist quinpirole. Prior studies indicate that MSN-MSN lateral connections are acutely regulated by dopamine[47,48] and D2-D1 connections specifically are inhibited by the D2R agonist quinpirole.[27,48] We replicated this finding in healthy animals and discovered that D2-D1 connections are also inhibited by quinpirole in parkinsonian animals and parkinsonian animals chronically treated with levodopa. In the LID state, a dopamine-mediated decrease in D2-D1 connectivity would be predicted to facilitate increases in both D1-MSN firing rates and ensemble sizes.

Synaptic transmission between MSNs has been described in organotypic cultures, the nucleus accumbens,[27,48] and in the dorsal striatum.[49,50,38,18] However, these studies cannot tell us the function of MSN-MSN interactions *in vivo*. A prior study in the nucleus accumbens found that both D2-D1 connections and cocaine-induced locomotor hyperactivity were dependent on dopamine D2R, but could not directly show that changes in lateral inhibition caused hyperactivity.[27] One obstacle to identifying the behavioral role of MSN-MSN connections is that MSNs may regulate circuit function and behavior via local GABA release in the striatum and/or via their connections to downstream basal ganglia nuclei. Chemogenetic or optogenetic activation of D2-MSNs reduces the

behavioral response to levodopa, causally linking D2-MSNs to LID.[45,51] From this literature, it is unclear whether D2-MSNs regulate LID via local striatal connections, their output to GPe, or both. We took advantage of the lack of GIRK effectors[43,43,44] to inhibit MSN synaptic outputs in the striatum without affecting their overall firing or synaptic output downstream. To our knowledge, our study is the first to directly test the function of MSN-MSN connections *in vivo*. We found that disruption of D2-mediated lateral connections lowers the threshold for the expression of dyskinesia, and explains part of the overall effect of inhibiting D2-MSNs in dyskinesia. A caveat to our chemogenetic approach is that the manipulation targets a pre-synaptic cell type. Future work could utilize alternative techniques, such as drugs acutely restricted by tethering (DART)[52] to achieve post-synaptic specificity.

In many ways, the functional importance of striatal lateral inhibition in action selection is not surprising. In sensory systems, lateral inhibition plays a role in improving sensory perception by shaping the pattern of neural activity evoked by sensory stimuli.[19,20,21,22,23,24,25,26] Our work suggests a parallel role in the motor system: lateral inhibition may serve to limit the number of activated neurons and intensity of activation elicited by motor inputs. This system may promote the selection of desired actions while suppressing competing motor programs[53,10,54]. In fact, the anatomy of the striatum supports this model. MSNs have extensive axonal arborizations within the striatum, extending up to 0.5 mm [5511]. Although MSN-mediated connections have small unitary connection strengths, they form at rates up to 36%, and comprise >90% of all striatal neurons[2,18]. The sheer size of this inhibitory plexus and its spatial organization may have strong implications for shaping striatal output.

ACKNOWLEDGEMENTS

This work was supported by grants from the National Science Foundation (NSF GRFP 2034836 to E.L.T.), the National Institute of Neurological Disorders and Stroke (NINDS) (R01NS101354 to A.B.N.), Richard and Shirley Cahill Endowed Chair in Parkinson's Disease Research (to A.B.N.). Additionally, this research was funded in part by Aligning Science Across Parkinson's (ASAP020529 to A.B.N.) through the Michael J. Fox Foundation for Parkinson's Research (MJFF). For the purpose of open access, the author has applied a CC BY public copyright license to all Author Accepted Manuscripts arising from this submission. We thank Drs. Massimo Scanziani, Kevin Bender, and Felice Dunn and all members of the Nelson Lab for helpful feedback on the project and manuscript.

AUTHOR CONTRIBUTIONS

Conceptualization, E.L.T. and A.B.N.; Methodology, E.L.T., C.J.B.M., & A.B.N.; Investigation, E.L.T., L.S., C.J.B.M., A.E.G., S.S., and A.B.N.; Formal Analysis, E.L.T. and A.B.N.; Writing – Original Draft, E.L.T. and A.B.N.; Writing – Review & Editing, all authors; Visualization: E.L.T. and A.B.N.; Funding Acquisition, E.L.T. and A.B.N.; Supervision, A.B.N.

SUPPLEMENTAL INFORMATION

Figure S1. *MSN-MSN lateral connections are mediated by $GABA_A$ receptors.*
Figure S2. *Unilateral depletion of dopamine causes rotational bias.*
Figure S3. *D1-D2 synaptic responses are not remodeled in parkinsonian animals and parkinsonian animals chronically treated with levodopa.*
Figure S4. *Chemogenetic inhibition of striatal lateral connections originating from D2-MSNs is not sufficient to cause dyskinesia without levodopa.*
Table S1. *Statistical table.*

METHODS

RESOURCE AVAILABILITY

Lead contact

Requests for additional information, resources, or reagents should be directed to and will be fulfilled by the Lead contact, Alexandra Nelson (alexandra.nelson@ucsf.edu).

Materials availability

This study did not generate any new unique materials.

Data and code availability

All data generated from this publication are available on Zenodo (DOI: 10.5281/zenodo.13917280). Any additional information required to reanalyze the data reported in this paper is available from the lead contact upon request. No new code was generated for this study.

EXPERIMENTAL MODEL AND STUDY PARTICIPANT DETAILS

Animals

All animal procedures were approved by the University of California San Francisco Institutional Animal Care and Use Committee (IACUC). Animals were housed under a 12h light/dark cycle with access to food and water ad libitum. For all experiments, both male and female C57Bl/6J mice, aged 3-12 months, were used. For *ex vivo* electrophysiology experiments, A2a-Cre;D1-tdTomato, D1-Cre;D1-tdTomato, and A2a-Cre;D2-GFP mice positive for both transgenes were used. For *in vivo* cannula infusion experiments, A2a-Cre animals were used. Age-matched littermates were randomly assigned to experimental and control groups.

METHOD DETAILS

Surgical Procedures

A detailed surgical protocol can be found at (DOI: dx.doi.org/10.17504/protocols.io.b9kxr4xn). Briefly, three- to six-month old mice were anesthetized with a combination of ketamine/xylazine (40/10 mg/kg IP) and inhaled isoflurane (1%). After placement in the stereotaxic frame (Kopf Instruments), the scalp was opened, and a mounted drill was used to create a hole over the left medial forebrain bundle (MFB). Using a 33-gauge needle (WPI) and Micro4 pump (WPI), 1 μL of 6-hydroxydopamine (6-OHDA, Sigma-Aldrich, 5 μg/μl in normal saline) was injected unilaterally into the MFB (-1.0 AP, -1.0 ML, -4.9 DV) at a rate of 0.2 μl/min. To reduce toxicity to other monoaminergic axons, desipramine (Sigma-Aldrich, 25mg/kg IP) was administered 30 min prior to 6-OHDA injection. Control animals were injected with 1 μL of normal saline in the MFB using the same parameters. After the operation, animals received daily saline injections and were provided high-fat dietary supplements (Diet-Gel, peanut butter, forage mix) for a 1-2 week recovery period.

Viral injections were performed during the same surgical procedure as the MFB injection described above. A mounted drill was used to create a hole over the left dorsolateral striatum (DLS). Using a 33-gauge needle (WPI) and a Micro4 pump (WPI), 1 µL of double-floxed inverse open reading frame (DIO) constructs were used to express virus in a pathway-specific manner. For *ex vivo* electrophysiology experiments, mice were injected with 1 µL AAV5-EF1a-DIO-hChR2-(H134R)-eYFP-wpre-HGH (1:3 dilution, Penn) into the left DLS (+0.8 AP, -2.3 ML, -2.5 DV). For chemogenetic inhibition experiments, mice were injected with 1 µL of AAV5-hSyn-DIO-hM4D(G_i)-mCherry (1:2 dilution, Addgene), or AAV5-hSyn-DIO-mCherry (undiluted, UNC) into the left DLS. For chemogenetic validation experiments, mice were injected with AAVs encoding both ChR2 and hM4Di.

For animals receiving local striatal infusions, the scalp was reopened 3–4 weeks after the initial surgeries to implant guide cannula assemblies in the DLS (5 mm pedestal with 0.05 mm protrusion; Protech International). Cannulas were secured in place with dental cement (Metabond) and dental acrylic (Ortho-Jet or Henry Schein).

Behavior

Details of the behavioral assessments can be found at (DOI: https://www.protocols.io/view/behavioral-testing-open-field-and-dyskinesia-scori-6qpvr67oovmk/v1). Gross movement was quantified across several metrics, using video-tracking software (Noldus Ethovision) of the animals in an open-field arena (25 cm diameter cylinder). Velocity, distance traveled, and rotational behavior were measured. Rotation rate was calculated in 60 s bins by subtracting total ipsilesional rotations from total contralesional rotations.

After a 3-week post-surgical baseline period, animals began daily treatment. Parkinsonian animals receiving levodopa developed robust levodopa-induced dyskinesia (LID). Dyskinesia was quantified using the Abnormal Involuntary Movement score (AIMs)[56], a standardized metric that takes into account dyskinesia across axial, limb, and orolingual body segments. As described by Cenci and Lunblad (2007), dyskinesia severity in each body segment was quantified during 60 s observation windows as follows: 0 = normal movement, 1 = abnormal movement for < 50% of the time, 2 = abnormal movement for > 50% of the time, 3 = abnormal movement for 100% of the time, but can be interrupted, and 4 = continuous, uninterruptable abnormal movement. The total AIM score represents the summation of the AIM score for each body segment (axial, limb, orolingual), for a maximum possible score of 12. For weekly scoring sessions, blinded experimenters rated AIMs every 20 m for a 2 h period. For cannula infusion experiments, dyskinesia was monitored every other minute.

Pharmacology

Details for the preparation of pharmacological agents can be found at (DOI: dx.doi.org/10.17504/protocols.io.261ge5yeyg47/v1). For *in vivo* experiments, levodopa (Sigma-Aldrich) was co-administered with benserazide (Sigma-Aldrich) and prepared in normal saline. For *ex vivo* electrophysiology experiments, 5–10 mg/kg levodopa and 2.5–10 mg/kg benserazide were used. Levodopa was given via IP injection 5–7 days per week. Daily levodopa injections continued for 3 or more weeks prior to experiments.

Clozapine N-Oxide (CNO) was dissolved in normal saline. CNO was delivered via local striatal infusion (10 μM) or via IP injection (1 mg/kg).

Prior to intracranial infusion experiments, a sub-dyskinetic dose of levodopa (0.75-2 mg/kg) was determined for each mouse. For the dose to be deemed sub-dyskinetic, the animal needed to display a prokinetic effect (contra-lesional rotational bias, increased velocity and distance traveled) with no dyskinesia (AIM score = 0). After the sub-dyskinetic doses were determined, the infusion experiments commenced. For infusion experiments, the experimenter was blinded to the viral construct injected in the mice. After a baseline period in the open-field arena, the dummy cannula was removed, and the infusion cannula was screwed into the guide. On interleaved days, CNO (10 mM) and saline were infused using a Hamilton syringe pump (WPI) at a rate of 0.2 μl/min for a total volume of 2 μl. The experimenter was also blinded to the infusion liquid. The infusion cannula was removed 10 min following the conclusion of the infusion and the dummy cannula was restored. Following a 10 min infusion baseline period, the mouse received an IP injection (sub-dyskinetic dose of levodopa or normal saline, delivered on interleaved days). Following IP injection, AIMs were monitored for 60 s every-other minute for 60 min. Infusion experiments were performed a minimum of 24 h apart.

To verify the placement and patency of the infusion cannulas, as well as the spread of the drug infusion, a lipophilic fluorescent dye (FM4-64x, Thermo-Fisher Scientific) was infused before sacrifice. The dye was infused using the same experimental parameters used for CNO infusion (2 μl at 0.2 μl/min). Fifteen min after the conclusion of the infusion, the animal was terminally anesthetized and transcardially perfused for immunohistochemistry.

For *ex vivo* experiments, picrotoxin (Sigma-Aldrich) was dissolved in warm water at 5 mM and added to ACSF for a final concentration of 50 μM. Quinpirole (Tocris) was dissolved in water and added to ACSF for a final concentration of 1 μM. CNO (Tocris) was dissolved in water at 10 mM and added to ACSF for final concentrations of 1 μM or 10 μM.

Ex vivo **electrophysiology**

A detailed protocol for *ex vivo* electrophysiology can be found at (DOI: dx.doi.org/10.17504/protocols.io.b9uir6ue). To prepare acute brain slices, mice were anesthetized with ketamine/xylazine and transcardially perfused with 95%O_2/5%CO_2 oxygenated, ice-cold glycerol-based artificial cerebrospinal fluid (ACSF) containing (in mM): 250 glycerol, 2.5 KCl, 1.2 NaH_2PO_4, 10 HEPES, 21 $NaHCO_3$, 5 D-Glucose, 2 $MgCl_2$, 2 $CaCl_2$. Following decapitation, brains were dissected and sequential coronal slices (275 μm) containing the striatum were collected with a vibratome (Leica). Slices were immediately transferred to a holding chamber containing warm (33°–34°C), carbogenated ACSF containing (in mM): 125 NaCl, 26 $NaHCO_3$, 2.5 KCl, 1.25 NaH_2PO_4, 12.5 D-Glucose, 1 $MgCl_2$, 2 $CaCl_2$. Slices were incubated for 30 min and then held at room temperature (22°–24°C) until used for recording.

For all recordings, slices were transferred to a recording chamber superfused (~2 mL/min) with carbogenated ACSF (31°–33°C). Medium spiny neurons were targeted for recordings using differential interference contrast (DIC) optics on an Olympus BX 51 WIF microscope. In Drd1a-tdTomato mice (Figures 1-3), direct pathway neurons were identified by their tdTomato-positive somata. Conversely, indirect pathway neurons were

identified by their medium-sized tdTomato-negative somata. In D2-GFP mice (Figure 4A-E), indirect pathway neurons were identified by their GFP-positive somata and direct pathway neurons were identified by their GFP-negative, medium-sized somata. Fluorescent-negative neurons with interneuron-like physiological properties were excluded from the dataset.

Medium spiny neurons were patched in the whole-cell configuration using borosilicate glass electrodes (2–5 MΩ). For voltage-clamp experiments, electrodes were filled with a cesium methanesulfonate-based internal solution with high chloride containing (in mM): 120 CsCl, 15 $CsMESO_3$, 8 NaCl, 0.5 EGTA, 10 HEPES, pH 7.3. For current-clamp experiments, electrodes were filled using a K-based internal solution containing (in mM): 130 $KMeSO_3$, 10 NaCl, 2 $MgCl_2$, 0.16 $CaCl_2$, 0.5 EGTA, 10 HEPES, 2 MgATP, 0.3 NaGTP, pH 7.3). After whole-cell break in, cells were given at least 5 min to dialyze internal solution before recording. Whole-cell recordings were made using a MultiClamp 700B amplifier (Molecular Devices) and digitized with an ITC-18 A/D board (HEKA). Data were acquired using Igor Pro 6.0 software (Wavemetrics) and custom acquisition routines (mafPC, courtesy of M.A. Xu-Friedman).

Inhibitory currents were optically evoked using 3 ms pulses of 473 nm light, ranging in power from 0.5-4 mW delivered by a TTL-controlled LED (Olympus) passed through a GFP filter (Chroma). Cells were voltage-clamped at -70 mV. Series resistance was monitored throughout the experiment, and cells were removed from analysis if the change in access was >20% from the baseline period. To determine if D1-MSNs had an intrinsic ChR2 current (in Drd1a-Cre animals injected with DIO-ChR2-eYFP), a 500 ms test pulse was delivered. Neurons with resulting 500 ms inward currents and/or response latency of <2 ms were deemed to have an intrinsic ChR2 current and excluded from further analysis. The same exclusion criteria were applied to D2-MSNs in Adora2a-Cre animals injected with DIO-ChR2-eYFP.

Histology and microscopy

A detailed protocol for preparation of histological sections can be found at (DOI: dx.doi.org/10.17504/protocols.io.b9ubr6sn). After behavioral or chemogenetic experiments, mice were anesthetized with ketamine/xylazine and transcardially perfused with 4% paraformaldehyde (PFA) in phosphate buffer solution (PBS). Following perfusion, brains were dissected and post-fixed overnight in 4% PFA, then transferred to 30% sucrose and stored at 4°C for cryoprotection. Brains were then sliced coronally into 30 µm sections on a freezing microtome (Leica).

After *ex vivo* electrophysiology experiments, 275 µm slices were stored overnight in 4% PFA. The following day, slices were transferred to 30% sucrose and sub-sectioned into 50 µm sections on a freezing microtome (Leica).

For immunohistochemistry, the tissue was blocked in 3% normal donkey serum (NDS) and permeabilized with 0.1% Triton X-100 on a room-temperature (RT) shaker. Primary anti-bodies (Rabbit anti-TH, Pel-Freez Biologicals, 1:1000) were added to the NDS and tissue was incubated overnight on a 4°C shaker. Tissue was then incubated in secondary antibodies (Donkey anti-rabbit Alexa Fluor 488 or 594, 1:500) overnight (16 h) on a 4°C shaker before being washed and mounted (Vectashield Mounting Medium) onto glass slides for imaging. Images (4x, 10x, or 40x) were obtained using a Nikon 6D conventional widefield microscope or an Olympus Fluoview FV3000 confocal

microscope. In 6-OHDA treated mice, the extent of dopamine depletion was confirmed by TH immunohistochemistry. Adequate expression of DIO constructs (ChR2-eYFP, eYFP, hM4D(G_i)-mCherry, mCherry) was confirmed.

QUANTIFICATION AND STATISTICAL ANALYSIS

Details can be found in Table S1. *Ex vivo* electrophysiology traces were processed in Igor Pro 6.3 (Wavemetrics). Statistical tests were performed using GraphPad Prism 10. All data are presented as the mean ± SEM, with “n” referring to the number of cells and “N” referring to the number of animals. Average amplitudes of oIPSCs collected using 1 mW light power were compared across MSN-MSN connection types (Figure 1G), as well as across treatment conditions (Figures 2G, 2I) using a nonparametric Kruskal-Wallis (KW) test. A post-hoc Dunn’s test for multiple comparisons was used. MSN-MSN oIPSC amplitudes following application of picrotoxin were compared using a paired, non-parametric Wilcoxon signed-rank (WSR) test (Figure S1). D2-D1 oIPSC amplitudes following application of quinpirole were also compared using a paired, non-parametric WSR for Ctrl, Park, and LD conditions (Figure 3D). The normalized oIPSC amplitude after application of quinpirole was compared across treatment conditions using a KW test (Figure 3D). A two-way repeated measures analysis of variance (2-way RM ANOVA) was used to compare AIMs score over time in systemic (IP injection) and infusion (cannula) chemogenetic inhibition experiments (Figures 4D, 4F).

References

1. Wilson, C. J. & Groves, P. M. Fine structure and synaptic connections of the common spiny neuron of the rat neostriatum: A study employing intracellular injection of horseradish peroxidase. *J. Comp. Neurol.* **194**, 599–615 (1980).
2. Graveland, G. A. & Difiglia, M. The frequency and distribution of medium-sized neurons with indented nuclei in the primate and rodent neostriatum. *Brain Res.* **327**, 307–311 (1985).
3. Jin, X., Tecuapetla, F. & Costa, R. M. Basal ganglia subcircuits distinctively encode the parsing and concatenation of action sequences. *Nat. Neurosci.* **17**, 423–430 (2014).
4. Barbera, G. *et al.* Spatially Compact Neural Clusters in the Dorsal Striatum Encode Locomotion Relevant Information. *Neuron* **92**, 202–213 (2016).
5. Cui, G. *et al.* Concurrent activation of striatal direct and indirect pathways during action initiation. *Nature* **494**, 238–242 (2013).
6. Parker, J. G. *et al.* Diametric neural ensemble dynamics in parkinsonian and dyskinetic states. *Nature* **557**, 177–182 (2018).
7. Sheng, M., Lu, D., Shen, Z. & Poo, M. Emergence of stable striatal D1R and D2R neuronal ensembles with distinct firing sequence during motor learning. *Proc. Natl. Acad. Sci.* **116**, 11038–11047 (2019).
8. Cruz, K. G. *et al.* Cortical-subcortical interactions in goal-directed behavior. *Physiol. Rev.* **103**, 347–389 (2023).
9. Mink, J. W. THE BASAL GANGLIA: FOCUSED SELECTION AND INHIBITION OF COMPETING MOTOR PROGRAMS. *Prog. Neurobiol.* **50**, 381–425 (1996).

10. Burke, D. A., Rotstein, H. G. & Alvarez, V. A. Striatal Local Circuitry: A New Framework for Lateral Inhibition. *Neuron* **96**, 267–284 (2017).
11. Tepper, J. M. *et al.* Heterogeneity and Diversity of Striatal GABAergic Interneurons: Update 2018. *Front. Neuroanat.* **12**, 91 (2018).
12. Gittis, A. H. *et al.* Rapid Target-Specific Remodeling of Fast-Spiking Inhibitory Circuits after Loss of Dopamine. *Neuron* **71**, 858–868 (2011).
13. Chang, H. T. & Kitai, S. T. Projection neurons of the nucleus accumbens: an intracellular labeling study. *Brain Res.* **347**, 112–116 (1985).
14. Somogyi, P., Bolam, J. P. & Smith, A. D. Monosynaptic cortical input and local axon collaterals of identified striatonigral neurons. A light and electron microscopic study using the golgi-peroxidase transport-degeneration procedure. *J. Comp. Neurol.* **195**, 567–584 (1981).
15. Taverna, S., Ilijic, E. & Surmeier, D. J. Recurrent Collateral Connections of Striatal Medium Spiny Neurons Are Disrupted in Models of Parkinson's Disease. *J. Neurosci.* **28**, 5504–5512 (2008).
16. Ryan, M. B., Bair-Marshall, C. & Nelson, A. B. Aberrant Striatal Activity in Parkinsonism and Levodopa-Induced Dyskinesia. *Cell Rep.* **23**, 3438-3446.e5 (2018).
17. Maltese, M., March, J. R., Bashaw, A. G. & Tritsch, N. X. Dopamine differentially modulates the size of projection neuron ensembles in the intact and dopamine-depleted striatum. *eLife* **10**, e68041 (2021).

18. Tecuapetla, F., Carrillo-Reid, L., Bargas, J. & Galarraga, E. Dopaminergic modulation of short-term synaptic plasticity at striatal inhibitory synapses. *Proc. Natl. Acad. Sci.* **104**, 10258–10263 (2007).
19. Dobbs, L. K. *et al.* Dopamine Regulation of Lateral Inhibition between Striatal Neurons Gates the Stimulant Actions of Cocaine. *Neuron* **90**, 1100–1113 (2016).
20. Liang, L., DeLong, M. R. & Papa, S. M. Inversion of Dopamine Responses in Striatal Medium Spiny Neurons and Involuntary Movements. *J. Neurosci.* **28**, 7537–7547 (2008).
21. Sagot, B., Li, L. & Zhou, F.-M. Hyperactive Response of Direct Pathway Striatal Projection Neurons to L-dopa and D1 Agonism in Freely Moving Parkinsonian Mice. *Front. Neural Circuits* **12**, 57 (2018).
22. Ryan, M. B. *et al.* Excessive firing of dyskinesia-associated striatal direct pathway neurons is gated by dopamine and excitatory synaptic input. *Cell Rep.* **43**, 114483 (2024).
23. Taverna, S., Van Dongen, Y. C., Groenewegen, H. J. & Pennartz, C. M. A. Direct Physiological Evidence for Synaptic Connectivity Between Medium-Sized Spiny Neurons in Rat Nucleus Accumbens In Situ. *J. Neurophysiol.* **91**, 1111–1121 (2004).
24. Taverna, S., Canciani, B. & Pennartz, C. M. A. Dopamine D1-Receptors Modulate Lateral Inhibition Between Principal Cells of the Nucleus Accumbens. *J. Neurophysiol.* **93**, 1816–1819 (2005).
25. Roth, B. L. DREADDs for Neuroscientists. *Neuron* **89**, 683–694 (2016).

26. Stachniak, T. J., Ghosh, A. & Sternson, S. M. Chemogenetic Synaptic Silencing of Neural Circuits Localizes a Hypothalamus→Midbrain Pathway for Feeding Behavior. *Neuron* **82**, 797–808 (2014).
27. Armbruster, B. N., Li, X., Pausch, M. H., Herlitze, S. & Roth, B. L. Evolving the lock to fit the key to create a family of G protein-coupled receptors potently activated by an inert ligand. *Proc. Natl. Acad. Sci.* **104**, 5163–5168 (2007).
28. Karschin, C., Dißmann, E., Stühmer, W. & Karschin, A. IRK(1–3) and GIRK(1–4) Inwardly Rectifying K^+ Channel mRNAs Are Differentially Expressed in the Adult Rat Brain. *J. Neurosci.* **16**, 3559–3570 (1996).
29. Liao, Y. J., Jan, Y. N. & Jan, L. Y. Heteromultimerization of G-Protein-Gated Inwardly Rectifying K^+ Channel Proteins GIRK1 and GIRK2 and Their Altered Expression in *weaver* Brain. *J. Neurosci.* **16**, 7137–7150 (1996).
30. Alcacer, C. *et al.* Chemogenetic stimulation of striatal projection neurons modulates responses to Parkinson's disease therapy. *J. Clin. Invest.* **127**, 720–734 (2017).
31. Tecuapetla, F., Matias, S., Dugue, G. P., Mainen, Z. F. & Costa, R. M. Balanced activity in basal ganglia projection pathways is critical for contraversive movements. *Nat. Commun.* **5**, 4315 (2014).
32. Fieblinger, T. *et al.* Cell type-specific plasticity of striatal projection neurons in parkinsonism and L-DOPA-induced dyskinesia. *Nat. Commun.* **5**, 5316 (2014).
33. Burke, D. A. & Alvarez, V. A. Serotonin receptors contribute to dopamine depression of lateral inhibition in the nucleus accumbens. *Cell Rep.* **39**, 110795 (2022).
34. Czubayko, U. & Plenz, D. Fast synaptic transmission between striatal spiny projection neurons. *Proc. Natl. Acad. Sci.* **99**, 15764–15769 (2002).

35. Tunstall, M. J., Oorschot, D. E., Kean, A. & Wickens, J. R. Inhibitory Interactions Between Spiny Projection Neurons in the Rat Striatum. *J. Neurophysiol.* **88**, 1263–1269 (2002).
36. Sáez, M. *et al.* D2 dopamine receptors and the striatopallidal pathway modulate L-DOPA-induced dyskinesia in the mouse. *Neurobiol. Dis.* **186**, 106278 (2023).
37. Shields, B. C. *et al.* Deconstructing behavioral neuropharmacology with cellular specificity. *Science* **356**, eaaj2161 (2017).
38. Angelucci, A. *et al.* Circuits and Mechanisms for Surround Modulation in Visual Cortex. *Annu. Rev. Neurosci.* **40**, 425–451 (2017).
39. DeAngelis, G. C., Robson, J. G., Ohzawa, I. & Freeman, R. D. Organization of suppression in receptive fields of neurons in cat visual cortex. *J. Neurophysiol.* **68**, 144–163 (1992).
40. Blakemore, C. & Tobin, ElisabethA. Lateral inhibition between orientation detectors in the cat's visual cortex. *Exp. Brain Res.* **15**, (1972).
41. Urban, N. Lateral inhibition in the olfactory bulb and in olfaction. *Physiol. Behav.* **77**, 607–612 (2002).
42. Wehr, M. & Zador, A. M. Balanced inhibition underlies tuning and sharpens spike timing in auditory cortex. *Nature* **426**, 442–446 (2003).
43. Foeller, E., Vater, M. & Kössl, M. Laminar Analysis of Inhibition in the Gerbil Primary Auditory Cortex. *J. Assoc. Res. Otolaryngol.* **2**, 279–296 (2001).
44. Kato, H. K., Asinof, S. K. & Isaacson, J. S. Network-Level Control of Frequency Tuning in Auditory Cortex. *Neuron* **95**, 412-423.e4 (2017).

45. Laskin, S. E. & Spencer, W. A. Cutaneous masking. II. Geometry of excitatory andinhibitory receptive fields of single units in somatosensory cortex of the cat. *J. Neurophysiol.* **42**, 1061–1082 (1979).
46. Mink, J. W. & Thach, W. T. Basal ganglia intrinsic circuits and their role in behavior. *Curr. Opin. Neurobiol.* **3**, 950–957 (1993).
47. Mink, J. W. The Basal Ganglia and Involuntary Movements: Impaired Inhibition of Competing Motor Patterns. *Arch. Neurol.* **60**, 1365 (2003).
48. Grofová, I. The identification of striatal and pallidal neurons projecting to substantia nigra. *Brain Res.* **91**, 286–291 (1975).
49. Cenci, M. A. & Lundblad, M. Ratings of L -DOPA-Induced Dyskinesia in the Unilateral 6-OHDA Lesion Model of Parkinson's Disease in Rats and Mice. *Curr. Protoc. Neurosci.* **41**, (2007).